The Canadian Mineralogist
Vol. 42, pp. 1683-1697 (2004)

GROWTH OF URANYL-HYDROXY-HYDRATE AND URANYL-CARBONATE MINERALS ON THE (104) SURFACE OF CALCITE

MICHAEL SCHINDLER§ AND FRANK C. HAWTHORNE

Department of Geological Sciences, University of Manitoba, Winnipeg, Manitoba R3T 2N2, Canada

CHRISTINE PUTNIS AND ANDREW PUTNIS

Institut für Mineralogie, Universität Münster, Corrensstr. 24, D-48149 Münster, Germany

ABSTRACT

Interaction of concentrated acidic uranyl-bearing solutions at initial values of pH of 2.5 and 4.5 with calcite at 25°C in an open system results in formation of schoepite, becquerelite and wyartite-II. Interaction of similar solutions with calcite at 100°C results in the formation of dehydrated schoepite after one day and becquerelite after two to three days. Concentrated basic uranyl-bearing solutions in contact with calcite at 25°C in an open system produce uranyl-bearing calcite, wyartite-II, becquerelite and schoepite. Uranyl tricarbonate minerals such as liebigite precipitate on calcite only in more highly concentrated basic solutions. The crystal morphologies of almost all of these minerals were recorded on the calcite surface with an atomic force microscope (AFM). Red crystals of becquerelite grown in acidic solutions are elongate parallel to [010], and the (001) face is defined by the [010], [110] and [100] edges. The (001) face of pink crystals of wyartite-II grown in an acidic solution is defined by the [120], [100] and [120] edges and has striations parallel to [100]. Under basic conditions, uranyl-bearing calcite precipitates as growth hillocks in the first few minutes of the experiments. Green crystals of liebigite are attached to the calcite surface *via* their (001) or (010) faces. The (001) face of pink-to-violet crystals of wyartite-II grown in basic solutions is defined by the [100], [110], [120], [230] and [010] edges. Small red crystals of becquerelite grown in basic solution have a similar morphology to those grown in acidic solution. The formation of wyartite-II is a result of high CO_2 activity on the calcite surface, which provides the necessary low values of Eh. The formation of schoepite on the calcite surface in Ca^{2+}–$(CO_3)^{2-}$ solutions occurs owing to favorable crystal-growth kinetics relative to becquerelite and other uranyl-carbonates. On the basis of observations in the open system, formation of minerals on the calcite surface is predicted for acidic and basic solutions in a closed system.

Keywords: uranyl minerals, crystal growth, calcite, surface.

SOMMAIRE

L'interaction de solutions concentrées acides d'uranyle à des valeurs initiales de pH de 2.5 et 4.5 avec la calcite à 25°C dans un système ouvert mène à la formation de schoepite, becquerelite et wyartite-II. L'interaction de solutions semblables avec la calcite à 100°C mène à la formation de schoepite déshydratée après un jour, et de becquerelite après deux ou trois jours. Des solutions à uranyle basiques et concentrées en contact avec la calcite à 25°C dans un système ouvert produisent la calcite uranylée, wyartite-II, becquerelite et schoepite. Les minéraux à uranyle tricarbonatés, tels la liebigite, se déposent sur la calcite seulement où les solutions basiques sont davantage concentrées. La morphologie des cristaux de la grande majorité de ces minéraux a été observée sur la surface de la calcite avec un microscope à force atomique (AFM). Les cristaux rouges de becquerelite germant dans un milieu acide sont allongés selon [010], et la face (001) est définie par les arêtes [010], [110] et [100]. La face (001) de cristaux roses de wyartite-II croissant dans un milieu acide est définie par les arêtes [120], [100] et [120], et montre des stries parallèles à [100]. En milieu basique, la calcite uranylée se dépose en amoncellements de croissance dans les premières minutes de l'expérience. Des cristaux verts de liebigite sont rattachés à la calcite sur leur face (001) ou (010). La face (001) de cristaux roses à violettes de wyartite-II croissant dans un milieu basique est définie par les arêtes [100], [110], [120], [230] et [010]. De petits cristaux rouges de becquerelite déposés dans un milieu basique ont une morphologie semblable à ceux que nous obtenons d'une solution acide. La formation de la wyartite-II résulte d'une activité élevée de CO_2 sur la surface de la calcite, qui fournit les faibles valeurs nécessaires de Eh. La formation de la schoepite sur la surface de la calcite en solutions contenant Ca^{2+} et $(CO_3)^{2-}$ est possible grâce à une cinétique de croissance cristalline favorable par rapport aux cas de la becquerelite et des autres carbonates uranylés. A la lumière des observations en système ouvert, nous prédisons la formation des minéraux sur la surface de la calcite dans des solutions acides et basiques en système fermé.

(Traduit par la Rédaction)

Mots-clés: minéraux à uranyle, croissance de cristaux, calcite, surface.

§ *E-mail address*: mschindl@lakeheadu.ca

Introduction

The development and evaluation of strategies for the long-term disposal of radioactive waste rely heavily on understanding the behavior of naturally occurring radionuclides. Uranium is the most abundant of the naturally occurring actinides and is one of the most toxic elements. In the tetravalent state, uranium is highly immobile; however, oxidation to U^{6+} results in the formation of the highly mobile uranyl ion, $(UO_2)^{2+}$. The mobility of the uranyl ion depends on its speciation at different pH, temperatures and solution compositions. In the absence of oxy-anion groups, such as $(PO_4)^{3-}$, $(SiO_4)^{4-}$, $(SO_4)^{2-}$, and humic acids, uranyl-hydroxy-hydrate and uranyl-carbonate complexes such as $[(UO_2)_3(OH)_5(H_2O)_5]^+$ and $[(UO_2)(CO_3)]^0$ are the dominant aqueous species. Uranyl-hydroxy-hydrate minerals are the most common group of uranyl minerals, and the concentration of U in natural solutions strongly depends on their stability. Here, we describe the results of *in situ* and batch crystal-growth experiments of uranyl-bearing minerals on the (104) calcite surface in the open system $CaO–Na_2O–UO_3–(CO_2)–H_2O$ at different values of pH.

Background Information

Solubility measurements on schoepite, $[(UO_2)_8O_2(OH)_{12}](H_2O)_{12}$, and becquerelite, $Ca[(UO_2)_3O_2(OH)_3]_2(H_2O)_8$, indicate that uranyl-hydroxy-hydrate minerals have their maximum stability between pH 5.5 and 8.0 (Torrero *et al.* 1994, Casas *et al*. 1997). In fresh water with high $p(CO_2)$ values, uranyl carbonate minerals precipitate from neutral to basic solutions. Less soluble uranyl carbonate sheet minerals such as rutherfordine, $[(UO_2)(CO_3)]$, and wyartite, $Ca[U^{5+}(UO_2)_2(CO_3)O_4(OH)](H_2O)_7$, crystallize from neutral solutions, and highly soluble uranyl di- and tricarbonates such as zellerite, $Ca[(UO_2)_2(CO_3)_2](H_2O)_5$, and liebigite, $Ca_2[(UO_2)(CO_3)_3](H_2O)_{11}$, crystallize through evaporation of weakly to strongly basic solutions (Finch & Murakami 1999). The concentration of $(UO_2)^{2+}$ in carbonate-rich groundwater with pH between 5.0 and 8.0 is controlled primarily by the presence of uranyl-hydroxy-hydrate and uranyl-carbonate sheet minerals. If solutions with lower and higher values of pH are neutralized through dissolution of carbonate minerals or atmospheric CO_2, these minerals precipitate and reduce the overall concentration of $(UO_2)^{2+}$ in aqueous solution. More highly concentrated uranyl-bearing solutions with pH below 5 or above 8 most likely occur in uranium mine- and mill-tailings, in which they interact with rock-forming minerals or barrier material. These interactions change the chemical composition, pH and Eh of the solution, and either uranium-bearing minerals precipitate or uranyl ions are adsorbed on the surface of minerals or barrier material. In order to prevent contamination of soil, surface water and groundwater close to uranium mine- and mill-tailings, we need to understand these chemical processes, particularly with regard to the following issues:

(1) The possible paragenesis of uranyl minerals or uranium-bearing minerals that precipitate from these solutions on the surface of the solid.

(2) The chemical composition of these minerals and the potential incorporation of other radionuclides into their structure.

(3) The growth and dissolution processes of uranyl- and U-bearing minerals, *i.e.*, the change in kinetics of growth or dissolution mechanisms with conditions in solution (*e.g.*, Eh, P, T, pH).

The Interaction of Calcite with U^{6+}-Bearing Solutions: Previous Work

Kitano & Oomori (1971) and Meece & Benninger (1993) showed that U^{6+} is preferentially incorporated into aragonite relative to calcite. Reeder *et al.* (2000) reported that aragonite and calcite can coprecipitate with up to 10000 and 1900 ppm U^{6+}, respectively, from aqueous solution. Reeder *et al.* (2001) examined the incorporation of uranyl carbonate species into calcite at pH values of 7.6 and 8.2, and showed that the dominant mechanism of growth during coprecipitation of calcite with $(U^{6+}O_2)^{2+}$ is spiral growth on the (104) face of calcite. The growth spirals form polygonal hillocks of four vicinal faces that differ in orientation of their growth edges and direction of growth. Uranyl carbonate is preferentially incorporated onto those vicinal faces, which are composed of an array of the (parallel and structurally identical) growth edges $[\bar{4}41]$ and $[48\bar{1}]$. The geometry and surface or bulk symmetry relations of the spiral-growth hillocks were described by Staudt *et al.* (1994), Paquette & Reeder (1995), Reeder (1996) and Reeder & Rakovan (1999), and the growth mechanisms of the spirals were observed *in situ* by atomic force microscopy (Gratz *et al.* 1993, Teng *et al.* 1998).

Using extended X-ray absorption fine-structure spectroscopy (EXAFS), X-ray photoelectron spectroscopy (XPS), and time-resolved laser-induced fluorescence spectroscopy (TXRLFS), Geipel *et al.* (1997) and Yu *et al*. (1998) showed that coatings of uranyl hydroxide and uranyl carbonate form on the surface of carbonate minerals upon interaction with a uranyl-bearing aqueous solution. Caroll *et al.* (1992) examined interactions at the calcite – uranyl solution interface, and observed precipitation of an unidentified Ca–uranyl compound on calcite; the morphologies of the crystals are different at pH values of 4.3 and 8.0. Glatz *et al.* (2002) synthesized becquerelite, $Ca[(UO_2)_4O_3(OH)_4](H_2O)_2$, and a third unidentified phase, through interaction of an acidic uranyl-bearing solution (at pH values of 4 and 6) with calcite between 140 and 220°C. In a recent paper, Schindler & Putnis (2004) described the growth of schoepite on the (104) face of calcite, and showed that

at constant temperature, the morphology of the schoepite crystals changes with variation in supersaturation and pH of the nascent solution.

Uranyl Oxide Minerals in the System $CaO–Na_2O–UO_3–(CO_2)–H_2O$

The system $CaO–Na_2O–UO_3–(CO_2)–H_2O$ system is one of the more complicated uranyl–aqueous systems. There at least seventeen uranyl-bearing minerals and three synthetic uranyl-bearing phases that can crystallize from aqueous solution (Table 1). Finch & Murakami (1999) presented an activity–activity diagram for the system $CaO–UO_3–(CO)_2–H_2O$ based on calculated and estimated Gibbs free energies. The diagram included only the more common uranyl-bearing minerals such as rutherfordine, schoepite, becquerelite, fontanite, sharpite and becquerelite, and indicated that the minerals with the largest fields of stability in this system are rutherfordine, schoepite and becquerelite.

Construction of an activity–activity diagram

In order to visualize the occurrence of all uranyl-oxide hydroxy-hydrate and uranyl carbonate phases in the system $CaO–UO_3–(CO_2)–H_2O$, one can calculate an activity–activity diagram for log [Ca] / $[H]^2$ *versus* log $[H_2CO_3]$ (Figs. 1a, 2a). The construction of such diagrams has been described in detail by Schindler & Hawthorne (2001). All minerals and synthetic phases in this diagram are related *via* different combinations of the general equations

$$\{M^{2+}{}_n \text{ interstitial complex}\}^{z+} = [(UO_2)_k O_l(OH)_m]^{z-} + a(H_2O) + b\{M^{2+}\} \leftrightarrow \{M^{2+}{}_{n+b} \text{ interstitial complex}\}^{(z+2b)} + [(UO_2)_k O_{l-a+b}(OH)_{m+2a-2b}]^{(z+2b)-} + 2bH^+ \quad [1]$$

$$\{M^{2+}{}_n \text{ interstitial complex}\}^{z+}[(UO_2)_k O_l(OH)_m(CO_3)_n]^{z-} + a\{M^{2+}\} + bH_2CO_3 \leftrightarrow \{M^{2+}{}_{n+a} \text{ interstitial complex}\}^{(z+2a)}[(UO_2)_k O_{l+a}(OH)_{m-2b}(CO_3)_{n+b}]^{(z+2a)-} + 2aH^+ + 2b–a(H_2O) \quad [2]$$

$$\{M^{2+}{}_n \text{ interstitial complex}\}^{z+}[(UO_2)_k O_l(OH)_m(CO_3)_n]^{z-} + bH_2CO_3 \leftrightarrow \{M^{2+}{}_{n+a} \text{ interstitial complex}\}^{(z+)}[(UO_2)_k O_l(OH)_{m-2b}(CO_3)_{n+b}]^{z-} + 2b(H_2O). \quad [3]$$

Similar to the construction of activity–activity diagrams for borate and uranyl-hydroxy-hydrate minerals (Schindler & Hawthorne 2001, 2004), these (and variations of these) general equations do not take into account the number of interstitial (H_2O) groups. Furthermore, we did not consider variation in the valence states of uranium in the structural unit for calculation of the boundary lines in the topology diagram. However, in later diagrams, we indicate minerals containing uranium in different valence states.

From the law of mass action, we may write the following relations for all equations:

$$\log [M^{2+}] / [H]^2 = \log K \quad (1)$$

$$\log [M^{2+}] / [H]^2 = a / b \log [H_2CO_3] + \log K \quad (2)$$

$$b [H_2CO_3] = \log K \quad (3)$$

We do not know log K, and hence the calculated values are only on a relative basis. However, the slope of the boundary between stability fields is given by either a / b, 0 or b (which we do know), and hence we can construct an activity–activity diagram with the correct topology. Figures 1a and 2a show the stability fields of the structural units and indicate the corresponding minerals and the chemical compositions of the structural units.

Minerals with U^{4+} and U^{5+}, such as ianthinite, $[U^{4+}{}_2(U^{6+}O_2)_4O_6(OH)_4\ (H_2O)_4](H_2O)_5$, wyartite, $Ca[U^{5+}(U^{6+}O_2)_2(CO_3)O_4(OH)](H_2O)_7$, and wyartite-II (unpublished) can only be stable at low redox potential, where U^{4+} and U^{5+} ions are stable in aqueous solution [*Eh* must be below 0.20 eV for U^{5+}; Langmuir (1978)]. Let us consider a hypothetical three-dimensional activity–activity diagram with the change in Eh in the third dimension. In this diagram, parts of the stability fields of the structural units of ianthinite, wyartite and wyartite-II will be at lower Eh than the stability fields of structural units with only U^{6+} present. For example,

TABLE 1. URANYL-OXIDE MINERALS AND SYNTHETIC PHASES IN THE SYSTEM $CaO–Na_2O–UO_3–(CO_2)–H_2O$

Mineral name	Formula	Ref.
Schoepite	$[(UO_2)_8O_2(OH)_{12}](H_2O)_{12}$	(1)
Metaschoepite	$[(UO_2)_8O_2(OH)_{12}]$	(2)
Dehydrated schoepite	$[(UO_2)O_{0.25-x}(OH)_{1.5+2x}]$, $0 < x < 0.25$	(3)
Becquerelite	$Ca[(UO_2)_3O_2(OH)_3]_2(H_2O)_8$	(4)
Ianthinite	$[U^{4+}{}_2(UO_2)_4O_6(OH)_4(H_2O)_4](H_2O)_5$	(5)
Wyartite	$Ca[U^{5+}(UO_2)_2(CO_3)O_4(OH)](H_2O)_7$	(6)
Fontanite	$Ca[(UO_2)_3(CO_3)_2O_2]H_2O)_6$	(7)
Blatonite	$(UO_2CO_3)(H_2O)$	(8)
Joliotite	$(UO_2CO_3)(H_2O)_2$	(9)
Zellerite	$Ca(UO_2)(CO_3)_2(H_2O)_5$	(9)
Metazellerite	$Ca(UO_2)(CO_3)_2(H_2O)_n$	(9)
Oswaldpeetersite	$[(UO_2)_2(CO_3)(OH)_2](H_2O)_4$	(10)
Urancalcarite	$Ca_2(UO_2)_3(CO_3)_5(OH)_6(H_2O)_5$	(11)
Sharpite	$Ca(UO_2)_6(CO_3)_5(OH)_4(H_2O)_6$	(12)
Liebigite	$Ca_2[(UO_2)(CO_3)_3](H_2O)_{11}$	(13)
Andersonite	$Na_2Ca[(UO_2)(CO_3)_3](H_2O)_5$	(14)
Čejkaite	$Na_4[(UO_2)(CO_3)_3]$	(15)
Synthetic	$Ca_{1-x}Na_{0.65}[(UO_2)(CO_3)_3](H_2O)_{n\ 38}$	(16)
Synthetic	$Ca[(UO_2)_4O_3(OH)_4](H_2O)_2$	(17)
Synthetic	α–$[UO_2(OH)_2]$	(18)

(1) Finch *et al.* (1996), (2) Weller *et al.* (2000), (3) Finch *et al.* (1998), (4) Pagoaga *et al.* (1987), (5) Burns *et al.* (1997), (6) Burns & Finch (1999), (7) Hughes & Burns (2003), (8) Vochten & Deliens (1998), (9) Finch & Murakami (1999), (10) Vochten *et al.* (2001), (11) Deliens & Piret (1984), (12) Čejka et al. (1984), (13) Mereiter (1982), (14) Mereiter (1986), (15) Li *et al.* (2001), Ondruš *et al.* (2003), (16) Vochten *et al.* (1994), (17) Glatz *et al.* (2002), (18) Taylor & Hurst (1971).

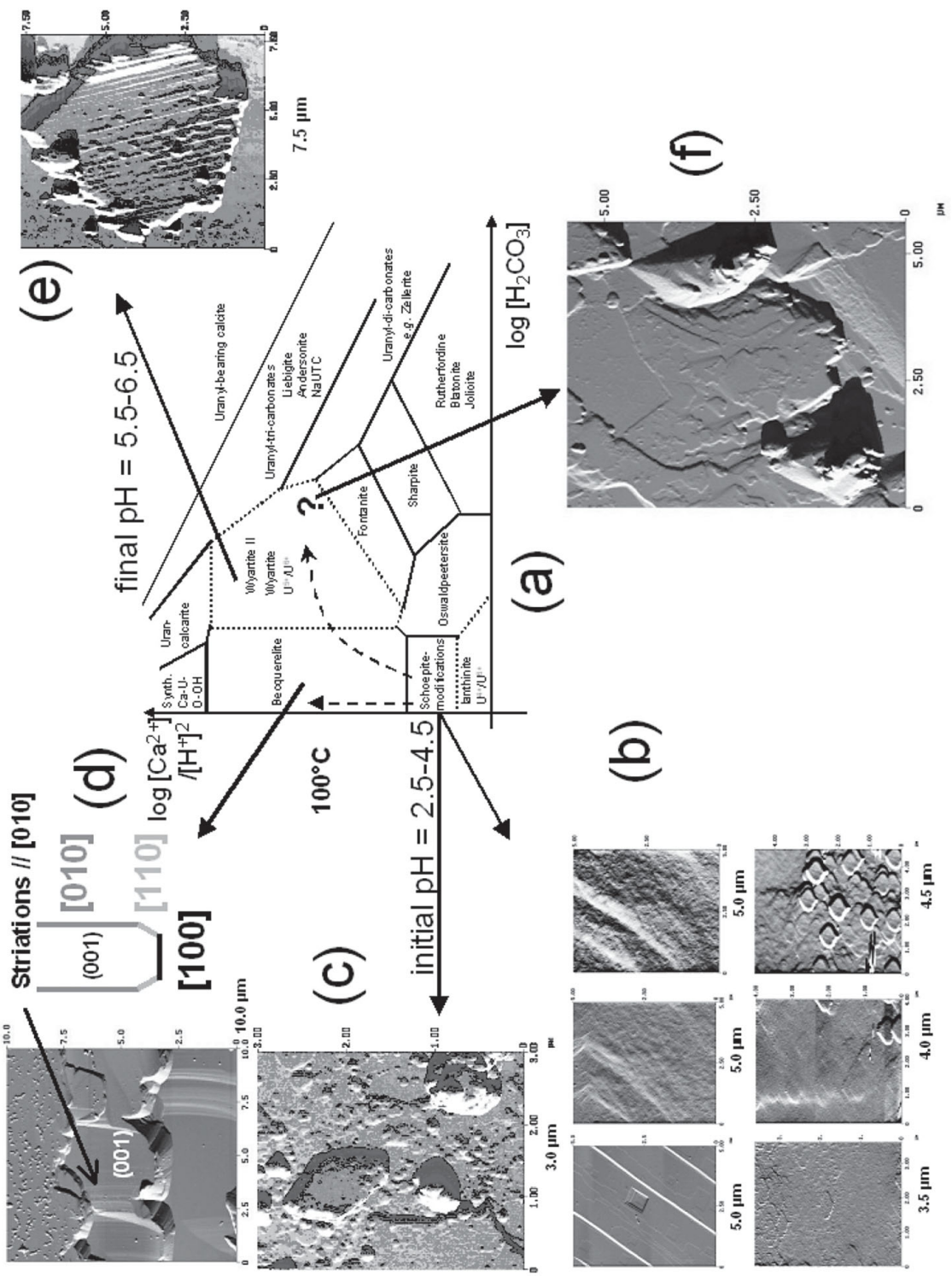
Striations // [010]
(001)
[010]
[110]
[100]
(d)
log [Ca2+]/[H+]2
final pH = 5.5-6.5
initial pH = 2.5-4.5
100°C
(c)
(a)
log [H2CO3]
Synth. Ca-U-O-OH
Uran-calcarite
Becquerelite
Uranyl-bearing calcite
Uranyl-tri-carbonates
Liebigite
Andersonite
NaUTC
Wyarite II
Wyarite
U4+/U6+
Schoepite-modifications
Ianthinite
U4+/U6+
Oswaldpeetersite
Fontanite
Sharpite
Uranyl-di-carbonates
e.g. Zellerite
Rutherfordine
Blatonite
Jolioite
?
(e)
7.5 µm
(f)
(b)
10.0 µm
3.0 µm
5.0 µm
5.0 µm
4.0 µm
4.5 µm
3.5 µm

becquerelite and wyartite are related *via* the chemical equation:

$$Ca(H_2O)_n[(UO_2)_3O_2(OH)_3]_2 + 2[H_2CO_3] + Ca^{2+} \leftrightarrow Ca_2(H_2O)_n[U^{5+}(UO_2)_2(CO_3)O_4(OH)]_2 + 2e^- + 4H_2O$$

The corresponding Nernst equation is

$$Eh = E_0 + 0.05916/2 \log \{[H_2CO_3]^2 [Ca^{2+}]\} \quad [4].$$

In a three-dimensional phase diagram showing log $[M^{2+}] / [H^+]^2$ *versus* log $[H_2CO_3]$ and *versus* Eh, the corresponding slope of the boundary between the stability fields is

$$\log [H_2CO_3] = Eh/0.05916 - E_0/0.05916 \quad [5].$$

Projecting this boundary line in a two-dimensional diagram showing log $[M^{2+}] / [H^+]^2$ *versus* log $[H_2CO_3]$ would result in a straight line parallel to the log $[M^{2+}] / [H^+]^2$ axis. This line and all other boundary lines between stability fields of structural units containing U^{6+} and U^{5+}–U^{6+} are shown as dotted lines in Figures 1a and 2a.

Experimental

Growth of uranyl-bearing minerals on the calcite (104) surface was examined after batch or *in situ* experiments using a Nanoscope III multimode scanning-probe microscope and a Dimension 3000 atomic force Microscope, both from Digital Instruments. The *in situ* experiments were done in a fluid cell from Digital Instruments. The calcite samples were freshly cleaved from a block of optically clear Iceland spar. The *in situ* experiments were free-drift: after injection of the solution into the fluid cell, the fluid flow was stopped while the images of the growth or dissolution experiments were recorded. The general scanning modes were contact and tapping.

FIG. 1. (a) Activity–activity diagram of log $[Ca^{2+}] / [H]^2$ *versus* log $[H_2CO_3]$ for uranyl-oxide minerals in the system $CaO–UO_3–(CO_2)–H_2O$. Possible sequences of minerals developed during interaction of acidic uranyl-bearing solutions with calcite at 25 and 100°C are indicated by broken arrows. Initial and final values of pH for the experiments are given on the left and at the top of the diagram. (b) AFM images of *in situ* crystal growth of schoepite in an acidic uranyl nitrate solution with an initial pH of 2.5 (Schindler & Putnis 2004). (c) AFM image of a single crystal of schoepite formed on the (104) surface of calcite after a three-day batch experiment with uranyl acetate solution of initial pH 4.5 (Schindler & Putnis 2004). (d) AFM image of rows of elongate crystals of becquerelite along [010] formed at 100°C in uranyl nitrate solution. The (001) faces of the crystals are defined by the [010], [100] and [110] edges. (e) AFM image of a single crystal of wyartite on calcite formed in a one-week batch experiment in uranyl acetate solution. (f) AFM image of single crystals of an unidentified phase formed during evaporation of uranyl acetate solution in contact with calcite.

Crystal-growth experiments of uranyl-bearing minerals in acidic solutions

The experiments were done with different molar ratios of uranyl nitrate or uranyl acetate. The concentrations of the uranyl salts varied between 1.5 and 100 mmol L^{-1}. Depending on the concentration, the starting pH of the uranyl nitrate solutions was approximately 2.5, and that of the uranyl acetate solutions, approximately 4.5. In the batch experiments, 30 mg of calcite (freshly cleaved from Iceland spar and crushed) was washed in distilled water and brought in contact with 5 mL of the solution. The size of the calcite crystals was approximately 3 × 3 [the (104) surface] × 2 mm. All batch experiments were done at 25°C in an open vessel with contact times between 2 and 7 days. At the end of each experiment, the pH was 5.5–6.0 for uranyl nitrate solutions and 6.0–6.5 for uranyl acetate solutions.

Crystal-growth experiments of uranyl-bearing minerals in basic solutions

The experiments under strongly basic conditions were done with different molar ratios of uranyl nitrate and Na_2CO_3, $Ca(OH)_2$ or $CaCl_2$–Na_2CO_3. The concentrations of uranyl nitrate were 0.5, 1, 5, 10 and 50 mmol L^{-1}. The molar ratios of uranyl nitrate : Na_2CO_3, uranyl nitrate : $Ca(OH)_2$ and uranyl nitrate : $CaCl_2$: Na_2CO_3 were in all cases 1 : 4, 1 : 2 and 1 : 2 : 3, with maximum concentrations of 50 mmol L^{-1} $(UO_2)(NO_3)_2$, 100 mmol L^{-1} $CaCl_2$, and 150 mmol L^{-1} Na_2CO_3. At the beginning of each experiment, 30 mg of freshly washed crystals of calcite was brought into contact with 5 mL of the corresponding solution in an open vessel. The starting pH was in all cases between 9.5 and 10.5, and the final pH was between 7.5 and 8.0. All batch experiments were done at 25°C with contact times between 2 days and 3 months.

Identification of uranyl-bearing minerals on the surface of calcite

After *in situ* or batch experiments, the uranyl minerals were scraped from the calcite surface and analyzed by X-ray powder diffraction with a Philips PW3040 diffractometer. The minerals were also examined by scanning electron microscopy (SEM) and semi-quantitative chemical analysis with a JEOL JSM–6300F microscope and an EDAX system from Oxford Instru-

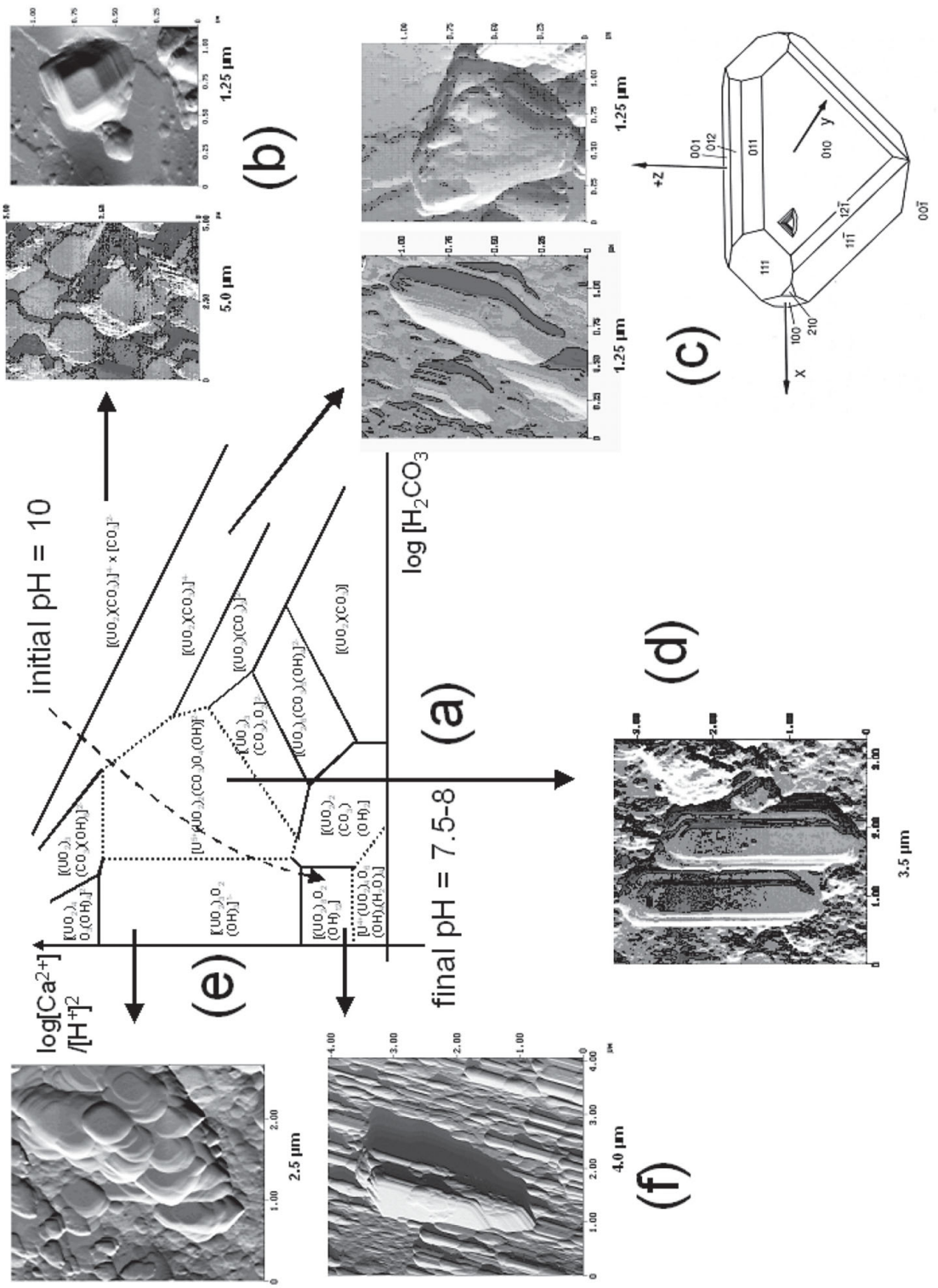
initial pH = 10
final pH = 7.5-8
log [H2CO3]
log[Ca2+]/[H+]2
(a)
(b)
(c)
(d)
(e)
(f)
1.25 µm
5.0 µm
2.5 µm
4.0 µm
3.5 µm
+z
y
x
001
012
011
010
111
100
210

ments. Thermogravimetric analysis of the material was done with a Firma Mettler instrument. The surface of each calcite crystal was also examined by SEM and by reflected-light microscopy.

Most of the uranyl oxides can be clearly distinguished by their color and fluorescence. Schoepite and dehydrated schoepite crystals are usually yellow, wyartite and wyartite-II are violet to pink, ianthinite is violet, and andersonite and liebigite are green and show fluorescence. In Nature, becquerelite crystals are usually yellow. However, synthetic becquerelite on calcite (identified as becquerelite by scraping the orange-red crystalline material from the calcite surface and characterizing it by X-ray powder diffraction) appears orange to red on the calcite surface. Moreover, we could select specific areas on the (104) calcite surface with one particular phase. We scanned these areas with the AFM and obtained three-dimensional images of the crystals. The AFM images show much better resolution of crystal faces and striations on crystal faces than SEM images. The crystal habits and forms of crystal faces were then compared to the morphology of crystals from mineral samples or to drawings of crystal morphologies from the literature.

Growth of Uranyl-Oxide Minerals on Calcite under Acidic Conditions

Acidic uranyl-bearing solutions are usually undersaturated with respect to uranyl minerals. If these solutions come into contact with calcite, calcite begins to dissolve. This dissolution increases the pH of the solution and results in supersaturation with respect to uranyl minerals (Schindler & Putnis 2004). This process can be divided into three steps:

(a) Step 1: dissolution of calcite and increasing pH:

$$CaCO_3 + 2H^+ \leftrightarrow Ca^{2+} + H_2CO_3 \quad [6]$$

$$H_2CO_3 \leftrightarrow CO_2\ (\text{aqueous}) + H_2O \quad [7]$$

$$CO_2(aq) \leftrightarrow CO_2\ (\text{gaseous}) \quad [8]$$

(b) Step 2: polymerization of the aqueous $(UO_2)^{2+}$-bearing species to form more highly polymerized species:

$$3(UO_2)^{2+} + 5(H_2O) \leftrightarrow [(UO_2)_3(OH)_5]^+ + 5H^+ \quad [9]$$

$$(UO_2)^{2+} + HCO^-_3 \leftrightarrow [(UO_2)(CO_3)]_{eq} + H^+ \quad [10]$$

(c) Step 3: crystallization through polymerization of the aqueous species to form minerals (*e.g.*, schoepite):

$$8[(UO_2)_3(OH)_5]^+ + 14H_2O \leftrightarrow 3[(UO_2)_8O_2(OH)_{12}](H_2O)_{12} + 8H^+ \quad [11]$$

Contact of acidic uranyl acetate solutions (initial pH = 4.5, final pH in the range 6.5–7.0, initial concentrations 10–100 mmol L^{-1}) with calcite in an open system for one week at 25°C normally results in the formation of schoepite, becquerelite and wyartite.

The type of speciation depends on pH and the concentration of (H_2CO_3), *i.e.*, the amount of dissolved $CaCO_3$. Schindler & Putnis (2004) calculated for the *in situ* experiments the distribution of aqueous species for uranyl nitrate and uranyl acetate solutions by extrapolating the amount of dissolved H_2CO_3 *via* the observed changes in pH. Their calculations showed that in the first few minutes of the *in situ* experiments, the uranyl-hydroxy-hydrate aqueous species (98% of all species) are dominant over the uranyl carbonate species (maximum 2% of all species). However, the activity of uranyl carbonate species increases with increasing dissolution of calcite during the long-term batch experiments.

Formation of schoepite on calcite under acidic conditions

Schindler & Putnis (2004) showed that in the first few minutes of contact between acidic solutions and calcite, schoepite precipitates on the surface of calcite. Contact of calcite with strongly acidic uranyl nitrate solutions (initial pH = 2.5, final pH = 5.5) results in precipitation of schoepite, together with a large amount of X-ray-amorphous material. Figure 1b shows AFM images of the formation of a fine-grained layer on the calcite surface (upper images), on which small crystals of schoepite appear six to ten minutes after injection of the solution into the fluid cell (lower images; for details, see Schindler & Putnis 2004).

Contact of calcite with the more weakly acidic uranyl acetate solution (initial pH = 4.5, final pH = 6.5) precipitated schoepite of a higher crystallinity than

FIG. 2. (a) Activity–activity diagram of log $[Ca^{2+}] / [H]^2$ *versus* log $[H_2CO_3]$, showing the chemical composition of the structural units and the possible sequence of minerals developed during interaction of basic uranyl-bearing solutions with calcite at 25°C (arrows). The initial and final values of pH for the experiments are given at the top and bottom of the diagram. (b) AFM images of growth hillocks of uranyl-bearing calcite on calcite. (c)–(f) AFM images of uranyl-oxide minerals on the calcite surface formed in highly concentrated basic uranyl-bearing solutions (50 mmol L^{-1}). (c) Single crystals of liebigite in two different orientations: left, with the (001) face parallel to the surface of calcite; right, with (010) face parallel to the surface of calcite. (d) Elongate crystals of wyartite. (e) A pile of small crystals of becquerelite. (f) Schoepite crystals with the (100) face parallel to the surface of calcite (Schindler & Putnis 2004).

schoepite formed in uranyl nitrate solution over the same period of time (3 days). Figure 1c shows an AFM image of a typical idiomorphic crystal of schoepite on the calcite surface, formed after three- to seven-day batch experiments with uranyl acetate solutions (Schindler & Putnis 2004). Interaction of calcite with the same solutions at 100°C resulted in the formation of dehydrated schoepite (only in the first 24 h), and we did not observe any epitactic growth of dehydrated schoepite crystals on the calcite surface.

Formation of becquerelite on calcite under acidic conditions

Formation of becquerelite on the (104) calcite surface was not observed during *in situ* AFM experiments. Three- to seven-day batch experiments at 25°C with uranyl acetate solution result in the formation of small amounts of becquerelite on calcite. Figure 3a shows a fine-grained precipitate of wyartite-II (violet) on top of becquerelite (red) after a one-week batch experiment.

The occurrence of only becquerelite on calcite can be observed after a three-day batch experiment at 100°C, in which the earlier-formed dehydrated schoepite is completely transformed into becquerelite. Figure 1d shows an AFM image of rows of slightly elongate crystals of becquerelite formed on the surface of calcite. In Nature, becquerelite crystals are usually elongate parallel to [010], show striations on the (011) face parallel to [010], and their (001) face is defined by the [010], [110] and [100] edges (Palache *et al.* 1944, Schindler *et al.* 2004a, b). Close inspection of the AFM images shows that these morphological features are also observed on becquerelite crystals grown on the (104) surface of calcite: the crystals are elongate parallel to [010], they have striations parallel to [010], and the edges [010], [110] and [100] define the (001) face (Fig. 1d).

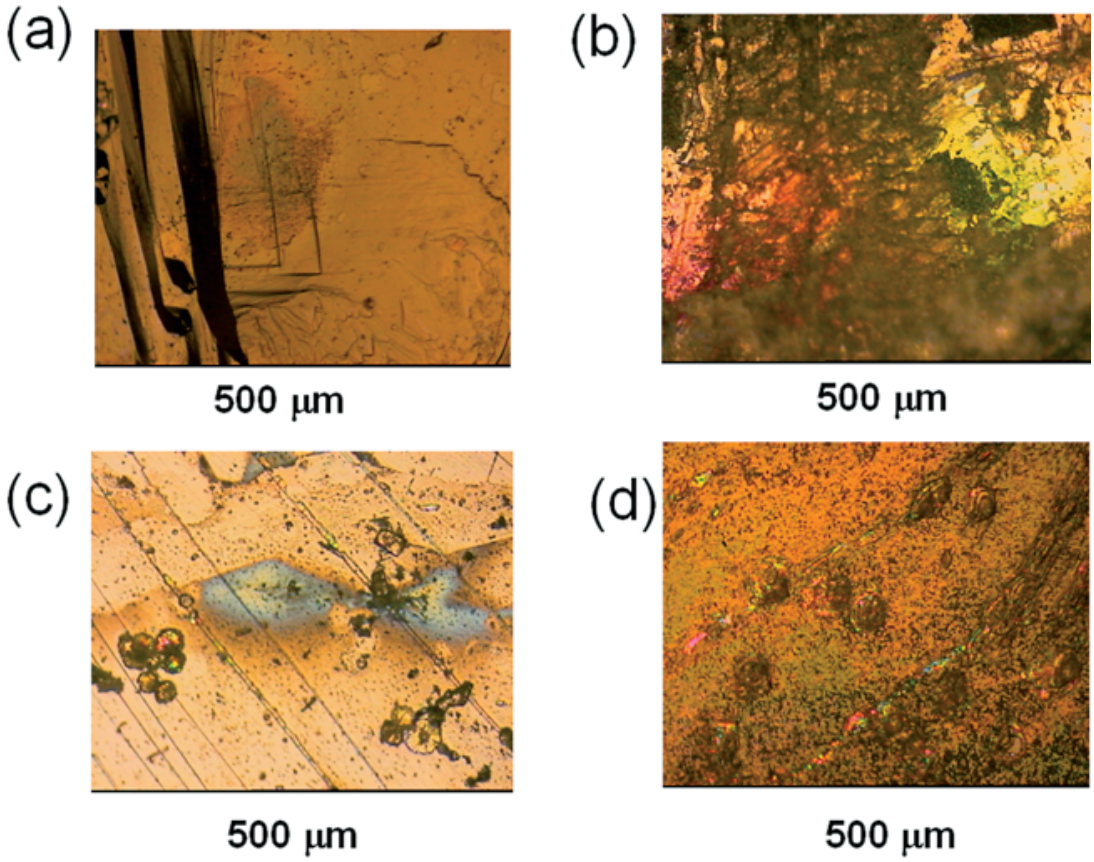

FIG. 3. Images taken with a reflection microscope: (a) wyartite (violet) and becquerelite (red) formed under acidic conditions. (b) Uranyl-bearing calcite (brown), becquerelite (red), schoepite (yellow) and liebigite (green) formed under basic conditions. (c) Fine-grained precipitate of wyartite formed under basic conditions, with an oxidized yellow core that subsequently forms in air. (d) Becquerelite (red) with liebigite (green) formed under basic conditions.

Formation of wyartite-II on calcite under acidic conditions

Wyartite-II is observed on the calcite surface after three- to seven-day batch experiments at 25ºC with uranyl acetate solutions (Fig. 3a). There are two different types of wyartite-II growth under acidic conditions: (1) a fine-grained violet precipitate on becquerelite (Fig. 3a), and (2) small pink single crystals on calcite. In the first case, AFM examination of the violet precipitate did not resolve any single crystals with well-defined morphologies. Figure 1e shows an AFM image of one of the pink single crystals of wyartite-II on calcite. The angles between the edges defining the (001) face indicate the occurrence of the [120], [100] and [110] edges (Fig. 4c). The (001) face is further characterized by striations parallel to [100] (Fig. 1c).

Formation of an unknown uranyl-carbonate phase on calcite

Partial evaporation of a uranyl acetate solution resulted in crystallization of an unknown greenish phase on calcite. The amount of material was too small for identification by X-ray diffraction, and the crystals do not exhibit a well-defined morphology (Fig. 1f). Formation during evaporation of a weak acidic solution indicates that this phase is presumably one of the highly soluble uranyl dicarbonate phases that are typical products of evaporation of near-neutral uranyl-bearing solutions (*e.g.*, Allen *et al.* 1995).

Sequence of formation of the observed phases under acidic conditions

Arrows in the activity–activity diagram (Fig. 1a) indicate the possible sequence of crystallization of

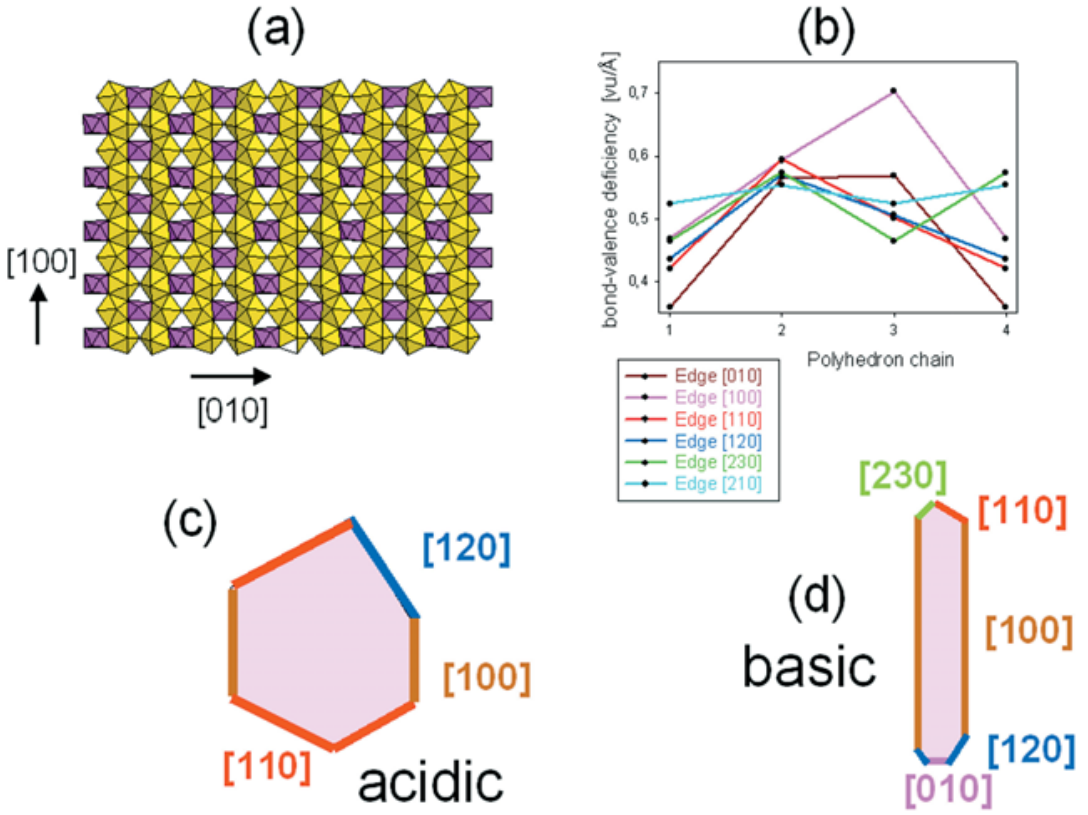

FIG. 4. (a) The structural unit in wyartite, with pentagonal bipyramids of U^{6+} (yellow) and U^{5+} (red). The carbonate triangles, which share edges with the U^{5+} pentagonal bipyramids, are omitted for clarity. (b) Calculated bond-valence deficiency per unit length [*vu* / Å] of anion terminations on chain terminations parallel to the edges [010], [100], [110], [120], [230] and [210]. (c), (d) Observed morphologies of the (001) face of wyartite crystals formed under acidic and basic conditions on calcite. The colors of the edges correspond to the colors in Figure 4c.

phases observed at 25 and 100°C under acidic conditions. Formation of becquerelite before wyartite-II is suggested by growth of wyartite on becquerelite or by replacement of becquerelite by wyartite-II (Fig. 3a). However, the exact sequence of the formation of these minerals remains unclear because we could not unequivocally determine if the observed single crystals of wyartite formed before or after the formation of becquerelite.

Growth of Uranyl-Oxide Minerals on Calcite under Basic Conditions

Yellow-brown uranyl-bearing calcite precipitated shortly after contact of a basic solution with calcite (Fig. 3b). In contact with calcite, uranyl-bearing solutions prepared with uranyl nitrate and Na_2CO_3 quickly became supersaturated with respect to uranyl-bearing calcite, and we observed *in situ* growth of uranyl-bearing calcite on calcite. Some of the solutions with $(UO_2)(NO_3)_2$, $CaCl_2$ and Na_2CO_3 were (presumably) already supersaturated with respect to uranyl-bearing calcite, and the latter precipitated even before the solution came into contact with calcite.

The formation of uranyl-bearing calcite can be expressed by the equation

$$y\mathrm{Ca}^{2+} + x[(\mathrm{U}^{6+}\mathrm{O}_2)(\mathrm{CO}_3)_3]^{4-} + y{-}2x(\mathrm{CO}_3)^{2-} \leftrightarrow \mathrm{Ca}_y(\mathrm{U}^{6+}\mathrm{O}_2)_x(\mathrm{CO}_3)_{x+y} \quad [12].$$

Here, aqueous uranyl tricarbonate $[(U^{6+}O_2)(CO_3)_3]^{4-}$ is the predominant species under strongly basic conditions (Langmuir 1978). Figure 2b shows two AFM images of growth hillocks of uranyl-bearing calcite on the calcite surface. Such growth hillocks normally form in more highly supersaturated solutions by two-dimensional nucleation (Land *et al.* 1997, Teng *et al.* 1998). Because of massive precipitation of uranyl-bearing calcite shortly after interaction of the solution with calcite, we never observed *in situ* growth of a uranyl oxide mineral directly on the surface of calcite. As shown in Figure 3b, uranyl oxide minerals formed in some cases below a crust of uranyl-bearing calcite. Uranyl oxide minerals may have formed earlier than we actually observed them with optical-reflection microscopy, and we cannot determine the relative timing of crystallization of the uranyl oxide minerals under basic conditions.

In basic uranyl-solutions with low concentrations of uranium (5–10 mmol L^{-1} uranyl nitrate), wyartite, becquerelite and schoepite formed in one to three weeks. Basic solutions with uranium concentrations up to 50 mmol L^{-1} uranyl nitrate resulted in a similar range of time for the formation of liebigite. AFM images reveal the presence of other uranyl tricarbonate minerals on the calcite surface, but there is always an insufficient amount of these phases present for them to be identified by X-ray powder diffraction when mixed with dominant wyartite, becquerelite and schoepite.

All experiments were done in an open system where the solution was exposed to the atmosphere. Simultaneous precipitation of uranyl-bearing calcite (equation [9]) and absorption of (CO_2) from the atmosphere (equations [4]–[6]) result in a decrease of pH from 10 to 8.0–8.5. If one assumes similar values of pH on the surface of calcite as in the bulk solution, all the above-listed uranyl oxide minerals started to form in the pH range 8.0–8.5. The final pH of the solution was in all cases between 7.5 and 8 (approximately three weeks after contact time).

Formation of liebigite under basic conditions

Greenish crystals of liebigite formed on the calcite surface in highly concentrated uranyl-bearing solutions. Because liebigite fluoresces an intense blue-green under short- and long-wave ultraviolet radiation (Vochten *et al.* 1993), assemblages of liebigite crystals could be located on the calcite surface using optical reflection microscopy and an ultraviolet light source. Figure 3b shows liebigite (green) with schoepite (yellow), becquerelite (red) and uranyl-bearing calcite (brown); Figure 3c shows liebigite with becquerelite on the calcite surface.

AFM images indicate that the morphology of liebigite crystals that grew on the calcite surface resembles that of synthetic single crystals that grew slowly in solutions of similar chemical composition (Fig. 2c; Mereiter 1987). The AFM images also show that liebigite crystals have various orientations on the calcite surface. The image on the left shows an epitactic growth of liebigite crystals on calcite (or on an earlier-formed uranyl oxide phase that is now concealed by the overlying liebigite). On the basis of angles between the faces, the crystals grew parallel to [001] with the (001) face attached to the surface (Fig. 2c). In the image on the right, the crystals grew with their (010) face parallel to the surface.

Formation of wyartite-II under basic conditions

Wyartite-II shows two different types of growth mechanism on calcite: (1) precipitation of a fine-grained violet powder, and (2) growth of pink to violet single crystals. Figure 3c shows a fine-grained violet precipitate of wyartite with a yellow core. In air, the size of this yellow core increases with time and is consistent with slow oxidation of U^{5+} to U^{6+}. Gauthier *et al.* (1989) identified the final product of this oxidation process as yellow schoepite and dehydrated schoepite. AFM images on the border between the yellow core and the violet rim indicate that neither oxidation nor transformation of wyartite into schoepite affects the surface topography at a nanometer scale. Figure 2d shows an AFM image of elongate crystals of wyartite. On the basis of the angles between the edges, the (001) face is defined by the [100], [110], [120], [230] and [010] edges (Fig. 4d).

Formation of becquerelite and schoepite under basic conditions

Again, becquerelite appears orange to red on the surface of calcite (Figs. 3b, d). Individual crystals of becquerelite are only observed in three-week batch experiments. Figure 2e shows an AFM image of a pile of small crystals of becquerelite; the crystals have a morphology similar to that of the larger crystals of becquerelite formed under acidic conditions at 100°C (Fig. 1d). Schindler & Putnis (2004) showed that schoepite crystals formed under basic conditions in three-week batch-experiments have a different morphology than crystals formed under acidic conditions in one-week batch-experiments (*cf.*, Figs. 2f, 1c). Schoepite crystals grown on the surface of calcite (or an earlier-formed phase) also show a different epitactic growth under basic conditions than under acidic conditions: crystals formed under acidic conditions grow with their basal (001) face parallel to the (104) calcite surface (Fig. 2f), whereas crystals formed under basic conditions grow with their (100) face parallel to the (104) calcite surface (Fig. 1c; Schindler & Putnis 2004).

Sequence of formation of the observed phases under basic conditions

Arrows in the activity–activity diagram (Fig. 2a) indicate the sequence of phases predicted to crystallize at 25°C under basic conditions. However, with optical and AFM observations, we could only verify the following observations:

(a) Uranyl-bearing calcite precipitates in the first few minutes of interaction;

(b) Liebigite forms only from more highly concentrated uranyl-solutions;

(c) Wyartite, becquerelite and schoepite begin to form when the pH drops below 8.5.

Discussion

The most surprising result of our experiments is the formation of wyartite-II on the surface of calcite. Wyartite-II is not common, but our experiments show that it forms easily during interaction of acidic and basic uranyl-bearing solutions with calcite. The stability of U^{5+} is restricted to Eh values below 0.20 eV (Langmuir 1978). One would expect Eh values in the range of 0.6–1.0 eV to occur in a solution in contact with the atmosphere over a longer period (a week or more) (Faure 1998).

The reduction of U^{6+} to U^{5+} in solution was presumably caused by the ongoing dissolution of calcite and the resulting higher activity of CO_2 (aqueous) on the calcite surface than in the near-surface part of the solution. On the basis of the chemical composition of the solution, this seems to be the only reasonable explanation for the occurrence of Eh values below 0.20 eV and the subsequent stabilization of wyartite-II. The corresponding redox reaction might be expressed by the following equation:

$$2[(UO_2)_3(OH)_5(H_2O)_5]^+ + 2Ca^{2+} + 3H_2O + 2CO_2 \leftrightarrow Ca_2(H_2O)_{14}[U^{5+}(UO_2)_2(CO_3)O_4(OH)]_2 + \tfrac{1}{2}O_2 + 6H^+ \quad [13]$$

In this reaction, $2(H_2O)$ decomposes into O_2 and $4H^+$ in order to provide the required electrons for the reduction of U^{6+}.

Occurrence of schoepite under acidic and basic conditions

Another surprise was the formation of schoepite on the calcite surface under acidic *and* basic conditions, because Schindler & Putnis (2004) showed that at a pH value of 6.5 and a concentration of 0.016 mmol L^{-1} Ca^{2+} (produced by the dissolution of calcite), the solution is supersaturated with respect to becquerelite and schoepite by $\beta = 10^{18.05}$ and $\beta = 13.77$, respectively. In the experiments under basic conditions, the activities of the Ca^{2+} and carbonate species were naturally very high because we used combinations of Na_2CO_3, $CaCl_2$ or $Ca(OH)_2$ as the starting chemical reagents. Hence, one might expect fontanite, $Ca[(UO_2)_3(CO_3)_2O_2]$ $(H_2O)_6$, and sharpite, $Ca(UO_2)_6(CO_3)_5(OH)_4(H_2O)_6$, to occur with becquerelite and uranyl-bearing calcite. Schindler & Putnis (2004) argued that kinetic effects control the formation of schoepite *versus* becquerelite. This is in accord with our crystal-growth experiments on calcite. Schoepite precipitates shortly after contact of an acidic solution with calcite at 25 and 100°C, whereas becquerelite forms only in long-term batch-experiments at 25°C or in two- to three-day batch-experiments at 100°C. Hence, schoepite is less stable under the conditions of our experiments than becquerelite (or other Ca–uranyl–carbonate minerals), but the kinetics of its crystal growth favor its precipitation relative to becquerelite or other uranyl carbonates.

Prediction of Parageneses in the Closed System $CaO–Na_2O–UO_3–(CO_2)–H_2O$

The occurrence of schoepite, becquerelite, wyartite-II, liebigite and uranyl-bearing calcite in an open system $CaO–Na_2O–UO_3–(CO_2)–H_2O$ at 25°C enables us to predict which kind of minerals would form in the analogous closed system using the activity–activity diagram shown as Figure 1 and equations [4]–[6].

Acidic conditions

In a closed system, there is no CO_2 (aqueous) ↔ CO_2 (gaseous) exchange, which would result in a saturated

solution with respect to carbonic acid (H_2CO_3) under acidic conditions. The dominant aqueous species under these conditions would most likely be H_2CO_3 and HCO_3^-, the uranyl-hydroxy-hydrate and the uranyl carbonate species. Furthermore, a high activity of H_2CO_3 will cause further dissolution of calcite (Faure 1998):

$$CaCO_3 + H_2CO_3 \leftrightarrow Ca^{2+} + 2HCO_3^- \quad [14].$$

In contrast to an open system with the equilibrium CO_2 (aqueous) $\leftrightarrow$ CO_2 (gaseous), the possible result in a closed system will be a solution supersaturated with respect to calcite. The degree of supersaturation would also depend on the type and amount of precipitated uranyl-bearing phases in the first few minutes of the reaction between the uranyl solution and calcite. However, the activity of aqueous $\{CO_2\}$ and carbonic acid will be much higher in a closed system than in an open system. Because of the activity of $[H_2CO_3]^o$, the change in composition of an acidic solution in contact with calcite does not follow the arrows in the activity–activity diagram (Fig. 1a). One would expect that the composition of the solution would be somewhere in the lower right corner of the activity–activity diagram. Therefore this chemical composition would favor the formation of minerals such as fontanite, sharpite and rutherfordine. Because of its favorable growth-kinetics, one would further expect precipitation of schoepite. These considerations are in agreement with the synthesis of rutherfordine in a closed system at elevated CO_2 pressure at 100°C (Vochten & Blaton 1999).

Basic conditions

If a uranyl nitrate + Na_2CO_3 solution of pH = 10 comes into contact with calcite in a closed system, calcite would dissolve because of the undersaturation of the solution with respect to calcite:

$$CaCO_3 \leftrightarrow Ca^{2+} + (CO_3)^{2-} \quad [15].$$

In a closed system, there is no dissolution of CO_2 from the atmosphere, and therefore the pH of the solution should not decrease in the same way as in an open system. Hence, the change in chemical composition of the solution will not follow the arrows in the activity–activity diagram (Fig. 2a). The chemical composition of the solution will be in the upper part of the activity–activity diagram. Depending on the initial concentration of uranium, we would expect precipitation of phases such as uranyl-bearing calcite, urancalcarite and perhaps wyartite-II, becquerelite and synthetic $Ca[(UO_2)_4O_3(OH)_4](H_2O)_2$.

Crystal Morphology and pH

Schindler *et al.* (2004a, b) developed a new approach to calculate the stability of edges on basal faces of uranyl-sheet minerals. They showed that the occurrence of edges on basal faces of uranyl-sheet minerals depends on the interaction of the corresponding anion-terminations with the aqueous solution at different pH and degrees of supersaturation. The structural parameter and chemical composition of the chains of polyhedra parallel to the edge, the arrangement of the interstitial complexes, and the shift between the layers control the degree of interaction between the anion terminations on an edge with complexes in aqueous solution. Schindler & Putnis (2004) used this approach to explain the change in morphology of schoepite crystals grown on the calcite surface under different conditions (Figs. 1c, 2f).

The change in crystal morphology of uranyl-sheet minerals with change in pH of the nascent solution can be also observed in AFM images of wyartite crystals formed under acidic and basic conditions (Figs. 1e, 2d, 4c, d). However, the wyartite sheet is much more complicated (both in composition and structure) than the schoepite sheet. It contains pentagonal bipyramids with U^{6+} and U^{5+} in [7]-coordination (Fig. 4a) and carbonate triangles that share edges with the U^{5+} pentagonal bipyramids (Burns & Finch 1999). The different chains of polyhedra in the wyartite sheet have distinct chemical compositions, and thus they interact differently with aqueous solutions. Hence, it is more difficult to predict the occurrence of edges with a change in pH or supersaturation for wyartite and wyartite-II than for schoepite. However, we want to show briefly how the factors discussed above can still be used to explain and predict the general occurrence of edges on the basal face of wyartite and wyartite-II crystals. Details of this structural approach to the morphology of uranyl-sheet minerals can be found in Schindler *et al.* (2004a, b).

Structural parameter and chemical composition of chains of polyhedra in the wyartite sheet

On a surface, anions such as $(OH)^-$ or O^{2-} bond to fewer cations than the corresponding anions in the bulk structure. The valence-sum rule (Brown 1981, Hawthorne 1994, 1997) requires that the sum of the bond valences incident at an anion must be equal to its valence. Depending on pH and the composition of the nascent solution, anions on the surface will be protonated or accept bonds from aqueous species. Protonation and acceptance of bonds from aqueous species are the results of an interaction of a surface anion with the aqueous solution. Thus, the higher degree of protonation or the higher the number of accepted bonds, the higher the interaction of the anion with the aqueous solution. The degree of protonation and the number of accepted bonds depend on the type of anion and on the number of bonds from the cations in the bulk structure to this specific anion. The higher the initial protonation and the more cations that bond to an anion, the lower

the additional bond-valence the anion requires through protonation or acceptance of bonds from aqueous species. One can express the interaction of anions at an edge with the aqueous solution by their bond-valence deficiency (calculated for no interaction with the nascent solution) along a terminating chain of polyhedra parallel to a specific edge. Figure 4b shows the variation in bond-valence deficiency per unit length [*vu* / Å] of anions along different chains parallel to edges defining the (001) face of wyartite and wyartite-II. In these calculations, we only considered the bond-valence deficiency of equatorial anions, which are ligands of the pentagonal bipyramids.

Chains with the lowest bond-valence deficiency are those chains in which the anions have the lowest interaction with the aqueous solution. The corresponding edge has a high stability and will most likely occur on the final morphology. Inspection of Figure 4b shows that a chain parallel to [010] has the lowest minimum in bond-valence deficiency and that the minimum in bond-valence deficiency increases from chains parallel to [110] and [120], to chains parallel to [100] and [230], to chains parallel to [210]. Based on these minima, one expects that edges such as [010], [110] and [120] should always occur on the final morphology of the (001) face.

Shift between the sheets and arrangement of interstitial complexes

Schindler *et al.* (2004a, b) showed that a shift between layers in uranyl-sheet minerals increases the interaction of anions at the edge with the aqueous solution. However, inspection of the wyartite structure shows that there is no shift between the layers. Moreover, Schindler *et al.* (2004a, b) showed that the arrangement of interstitial complexes in rows parallel to specific edges favors growth of crystals in that same direction. In wyartite, the interstitial Ca atoms are arranged parallel to the [100] edge. Hence, one would expect preferred growth of wyartite crystals parallel to this edge.

Comparison with the observed morphology of wyartite

Based on the minima of bond-valence deficiency of the chains (Fig. 4b) and the arrangement of the interstitial complexes, one would expect wyartite and wyartite-II crystals to be elongate parallel to [100] and with a (001) face defined primarily by the [100], [110] and [120] edges. This is exactly the case: crystals formed under both acidic and basic conditions are elongate parallel to [100], and the morphology of the (001) face is mainly defined by the [100], [110] and [120] edges (Figs. 4c, d).

Conclusions

Interaction of acidic and basic uranyl-bearing solutions with the (104) face of calcite in an open system at 25°C results in formation of uranyl minerals on the calcite surface. The crystallization sequence schoepite → becquerelite → wyartite-II occurs under acidic conditions; the crystallization sequence uranyl-bearing calcite → liebigite → wyartite-II → becquerelite → schoepite occurs under basic conditions. On the basis of these observed sequences, we can predict the occurrence of minerals expected if acidic and basic solutions come in contact with calcite in a closed system at 25°C. These would be schoepite, fontanite, sharpite and rutherfordine under acidic conditions, and uranyl-bearing calcite, urancalcarite and perhaps wyartite-II, becquerelite and synthetic $Ca[(UO_2)_4O_3(OH)_4](H_2O)_2$ under basic conditions. Finally, we show that the occurrence of observed edges on the (001) face of wyartite-II crystals is in accord with the new approach of Schindler *et al.* (2004a, b) to explain the morphology of uranyl-sheet minerals.

Acknowledgements

We thank two anonymous reviewers for their incisive comments, and editor Bob Martin for making us write in Canadian English. MS was supported by an Emmy Noether Fellowship from the Deutsche Forschungsgemeinschaft. FCH was supported by a Canada Research Chair in Crystallography and Mineralogy and a Discovery Grant from the Natural Sciences and Engineering Research Council of Canada.

References

Allen, P.G., Bucher, J.J., Clark, D.L., Edelstein, N.M., Ekberg, S.A., Gohdes, J.W., Hudson, E.A., Kaltsoyannis, N., Lukens, W.W., Neu, M.P., Palmer, P.D., Reich, T., Shuh, D.K., Tait, C.D. & Zwick, B.D. (1995): Multinuclear NMR, Raman, EXAFS, and X-ray diffraction studies of uranyl carbonate complexes in near-neutral aqueous solution. X- ray structure of $(C(NH_2)_3)_6((UO_2)_3(CO_3)_6)\bullet 6.5(H_2O)$. *Inorg. Chem.* **34**, 4797-4807.

Brown, I.D. (1981): The bond-valence method: an empirical approach to chemical structure and bonding. *In* Structure and Bonding in Crystals II (M. O'Keeffe & A. Navrotsky, eds.). Academic Press, New York, N.Y. (1-30).

Burns, P.C. & Finch, R.J. (1999): Wyartite: crystallographic evidence for the first pentavalent-uranium mineral. *Am. Mineral.* **84**, 1456-1460.

_____, _____, Hawthorne, F.C., Miller, M.L. & Ewing, R.C. (1997): The crystal structure of ianthinite, $[U^{4+}_2(UO_2)_4O_6(OH)_4(H_2O)_4](H_2O)_5$: a possible phase for Pu^{4+} incorporation during the oxidation of spent nuclear fuel. *J. Nucl. Mater.* **249**, 199-206.

CAROLL, S.A., BRUNO, J., PETIT, J.-C. & DRAN, J.C. (1992): Interaction of U(VI), Nd, and Th(IV) at the calcite–solution interface. *Radiochim. Acta* **58/59**, 245-252.

CASAS, I., BRUNO, J., CERA, E., FINCH, R.J. & EWING, R.C. (1997): Characterization and dissolution behaviour of a becquerelite from Shinkolobwe, Zaire. *Geochim. Cosmochim. Acta* **61**, 3879-3884.

ČEJKA, J., MRÁZEK, Z. & URBANEC, Z. (1984): New data on sharpite, a calcium uranyl carbonate. *Neues Jahrb. Mineral., Monatsh.*, 109-117.

DELIENS, M. & PIRET, P. (1984): L'urancalcarite, $Ca(UO_2)_3CO_3(OH)_6{\bullet}3H_2O$, nouveau minéral de Shinkolobwe, Shaba, Zaïre. *Bull. Minéral*. **107**, 21-24.

FAURE, G. (1998): *Principles and Applications of Geochemistry* (2nd ed.). Prentice Hall, Upper Saddle River, New Jersey.

FINCH, R.J., COOPER, M.A., HAWTHORNE, F.C. & EWING, R.C. (1996): The crystal structure of schoepite, $[(UO_2)_8O_2(OH)_{12}](H_2O)_{12}$. *Can. Mineral.* **34**, 1071-1088.

_____, HAWTHORNE, F.C.& EWING, R.C. (1998): Structural relations among schoepite, metaschoepite and "dehydrated schoepite". *Can. Mineral*. **36**, 831-845.

_____ & MURAKAMI, T. (1999): Systematics and paragenesis of uranium minerals. *In* Uranium: Mineralogy, Geochemistry and the Environment (P.C. Burns & R.J. Finch, eds.). *Rev. Mineral.* **38**, 91-179.

GAUTHIER, G., FRANÇOIS, A., DELIENS, M. & PIRET, P. (1989): Famous mineral localities: the uranium deposits of the Shaba region, Zaire. *Mineral. Rec.* **20**, 265-288.

GEIPEL, G., REICH, T., BRENDLER, V., BERNHARD, G. & NITSCHE, H. (1997): Laser and X ray spectroscopic studies of uranium–calcite interface phenomena. *J. Nucl. Mater.* **248**, 408-411.

GLATZ, R.E., LI, YAPING, HUGHES, K.A., CAHILL, C.L. & BURNS, P.C. (2002): Synthesis and structure of a new Ca uranyl oxide hydrate, $Ca[(UO_2)_4O_3(OH)_4](H_2O)_2$, and its relationship to becquerelite. *Can. Mineral.* **40**, 217-224.

GRATZ, A.J., HILLNER, P.E. & HANSMA, P.K. (1993): Step dynamics and spiral growth on calcite. *Geochim. Cosmochim. Acta* **57**, 491-495.

HAWTHORNE, F.C. (1994): Structural aspects of oxides and oxysalt crystals. *Acta Crystallogr.* **B50**, 481-510.

_____ (1997): Structural aspects of oxide and oxysalt minerals. *In* Modular Aspects of Minerals (S. Merlino, ed.). *Eur. Mineral. Union, Notes in Mineralogy* **1**, 373-429.

HUGHES, K.-A. & BURNS, P.C. (2003): A new uranyl carbonate sheet in the structure of fontanite, $Ca[(UO_2)_3(CO_3)_2O_2](H_2O)_6$. *Am. Mineral.* **88**,

KITANO, Y. & OOMORI, T. (1971): The coprecipitation of uranium with calcium carbonate. *J. Ocean. Soc. Japan* **27**, 34-42.

LAND, T.A, DE YOREO, J.J. & LEE, J.D. (1997): An in-situ AFM investigation of canavalin crystallization kinetics. *Surface Sci.* **384**, 136-155.

LANGMUIR, D. (1978): Uranium solution – mineral equilibria at low temperatures with applications to sedimentary ore deposits. *Geochim. Cosmochim. Acta* **42**, 547-569.

LI, YAPING, KRIVOVICHEV, S.V. & BURNS, P.C. (2001): The crystal structure of $Na_4(UO_2)(CO_3)_3$ and its relationship to schröckingerite. *Mineral. Mag.* **65**, 297-304.

MEECE, D.E. & BENNINGER, L.K. (1993): The coprecipitation of Pu and other radionuclides with $CaCO_3$. *Geochim. Cosmochim. Acta* **57**, 1447-1458.

MEREITER, K. (1982): The crystal structure of liebigite, $Ca_2UO_2(CO_3)_3{\bullet}{\sim}11H_2O$. *Tschermaks Mineral. Petrol. Mitt.* **30**, 277-288.

_____ (1986): Neue kristallographische Daten über das Uranmineral Andersonit. *Anz. Österr. Akad. Wiss. Math-Naturwiss. Kl.* **3**, 39-41.

_____ (1987): Hemimorphy of crystals of liebigite. *Neues Jahrb. Mineral., Monatsh*., 325-328.

MOLL, H., REICH, T. & SZABÓ, Z. (2000): The hydrolysis of dioxouranium (VI) investigated using EXAFS and ^{17}O-NMR. *Radiochim. Acta* **88**, 411-415.

ONDRUŠ, P., SKÁLA, R., VESELOVSKÝ, F., SEJKORA, J. & VITTI, C. (2003): Čejkaite, the triclinic polymorph of $Na_4(UO_2)(CO_3)_3$ – a new mineral from Jachymov, Czech Republic. *Am. Mineral*. **88**, 686-693.

PAGOAGA, M.K., APPLEMAN, D.E. & STEWART, J.M. (1987): Crystal structures and crystal chemistry of the uranyl oxide hydrates becquerelite, billietite, and protasite. *Am. Mineral.* **72**, 1230-1238.

PALACHE, C., BERMAN, H. & FRONDEL, C. (1944): *The System of Mineralogy* (7th ed.). John Wiley & Sons, New York, N.Y.

PAQUETTE, J. & REEDER, R.J. (1995): Relationship between surface structure, growth mechanism, and trace element incorporation in calcite. *Geochim. Cosmochim. Acta* **59**, 735-749.

REEDER, R.J. (1996): Interaction of divalent cobalt, zinc, cadmium, and barium with the calcite surface during layer growth. *Geochim. Cosmochim. Acta* **60**, 1543-1552.

_____, NUGENT, M., LAMBLE, G.M., TAIT, C.D. & MORRIS, D.E. (2000): Uranyl-incorporation into calcite and aragonite: XAFS and luminescence studies. *Environ. Sci. Tech.* **34**, 638-644.

_____, _____, TAIT, C.D., MORRIS, D.E., HEALD, S.M., BECK, K.M., HESS, W.P. & LANZIROTTI, A. (2001): Coprecipitation of uranium(VI) with calcite: XAFS, micro-XAS, and luminescence characterization. *Geochim. Cosmochim. Acta* **65**, 3491-3503.

_____ & RAKOVAN, J. (1999): Surface structural control on trace element incorporation during crystal growth. *In* Growth, Dissolution, and Pattern Formation in Geosystems (B. Jamtveit & P. Mekin). Kluwer Academic, Dordrecht, The Netherlands (143-162).

SCHINDLER, M. & HAWTHORNE, F.C. (2001): A bond valence approach to the structure, chemistry and paragenesis of hydroxy-hydrated oxysalt minerals. III. Paragenesis of borate minerals. *Can. Mineral.* **39**, 1257-1274.

_____ & _____ (2004): A bond-valence approach to the uranyl-oxide hydroxy-hydrate minerals: chemical composition and occurrence. *Can. Mineral*. **42**, 1601-1627.

_____, MUTTER, A., HAWTHORNE, F.C. & PUTNIS, A. (2004a): Prediction of crystal morphology of complex uranyl-sheet minerals. I. Theory. *Can. Mineral.* **42**, 1629-1649.

_____, _____, _____ & _____ (2004b): Prediction of crystal morphology of complex uranyl-sheet minerals. II. Observations. *Can. Mineral.* **42**, 1651-1666.

_____ & PUTNIS, A. (2004): Crystal growth of schoepite on the (104) surface of calcite. *Can. Mineral.* **42**, 1667-1681.

STAUDT, W.J., REEDER, R.J. & SCHOONEN, M.A.A. (1994): Surface structural controls or compositional zoning of SO_4^{2-} and SeO_4^{2-} in synthetic calcite single crystals. *Geochim. Cosmochim. Acta* **58**, 2087-2098.

TAYLOR, J.C. & HURST, H.J. (1971): The hydrogen atom locations in the α and β forms of uranyl hydroxides. *Acta Crystallogr.* **B27**, 2018-2022.

TENG, H.H., DOVE, P.M., ORNE, C.A. & DE YOREO, J.J. (1998): Thermodynamics of calcite growth: baseline for understanding biomineral formation. *Science* **282**, 724-727.

TORRERO, M.E., CASAS, I., DE PABLO, J., SANDINO, M.C.A. & GRAMBOW, B. (1994): A comparison between unirradiated UO_2(s) and schoepite solubilities in 1 m NaCl medium. *Radiochim. Acta* **66/67**, 29-35.

VOCHTEN, R. & BLATON, N. (1999): Synthesis of rutherfordine and its stability in water and alkaline solutions. *Neues Jahrb. Mineral., Monatsh.*, 372-384.

_____ & DELIENS, M. (1998): Blatonite, $UO_2CO_3 \cdot H_2O$, a new uranyl carbonate monohydrate from San Juan County, Utah. *Can. Mineral.* **36**, 1077-1081.

_____, _____ & MEDENBACH, O. (2001): Oswaldpeetersite, $[(UO_2)_2(CO_3)(OH)_2] \cdot 4(H_2O)$, a new basic uranyl carbonate mineral from the Jomach uranium mine, San Juan County, Utah, U.S.A. *Can. Mineral.* **39**, 1685-1689.

_____, VAN HAVERBEKE, L. & VAN SPRINGEL, K. (1993): Synthesis of liebigite and andersonite, and study of their behavior and luminescence. *Can. Mineral.* **31**, 167-171.

_____, _____, _____, BLATON, N. & PEETERS, O.M. (1994): The structure and physicochemical characteristics of a synthetic phase compositionally intermediate between liebigite and andersonite. *Can. Mineral.* **32**, 553-561.

WELLER, M.T., LIGHT, M.E. & GELBRICH, T. (2000): Structure of uranium(VI) oxide dihydrate, $UO_3 \cdot 2H_2O$; synthetic meta-schoepite $(UO_2)_4O(OH)_6 \cdot 5H_2O$. *Acta Crystallogr.* **B56**, 577-583.

YU, A., TETERIN, K.E., IVANOV, A.S., BAEV, S., NEFEDOV, V.I., GEIPEL, G., REICH, T. & NITSCHE, H. (1998): X-ray photoelectron study of the interaction of $UO_2(ClO_4)_2$ with calcite and diabase minerals in water solutions. *Surf. Invest.* **13**, 613-622.

Received November 3, 2003, revised manuscript accepted September 8, 2004.